Influence of the Crc regulator on the hierarchical use of carbon sources from a complete medium in *Pseudomonas*

Ruggero La Rosa[1], Volker Behrends[2,3], Huw D. Williams[4], Jacob G. Bundy[3], Fernando Rojo[1]

[1] Departamento de Biotecnología Microbiana, Centro Nacional de Biotecnología, CSIC, Darwin 3, Cantoblanco, 28049 - Madrid, Spain

[2] Department of Life Sciences, University of Roehampton, London SW15 4DJ, UK

[3] Department of Surgery and Cancer, Faculty of Medicine, Imperial College London, London SW7 2AZ, UK

[4] Department of Life Sciences, Faculty of Natural Sciences, Imperial College London, London SW7 2AZ, UK

* Correspondence: Prof. Fernando Rojo, Centro Nacional de Biotecnología, CSIC. Darwin 3, Cantoblanco, 28049 Madrid, Spain. E-mail: frojo@cnb.csic.es; Tel: (+34) 91 585 45 39; Fax: (+34) 91 585 45 06.

E-mail of co-authors: rlarosa@cnb.csic.es; Volker.Behrends@roehampton.ac.uk; j.bundy@imperial.ac.uk; h.d.williams@imperial.ac.uk

Running title: Crc and the hierarchy of substrate consumption

Key words: Global Regulation, Metabolism, Catabolite repression, metabolite profiling

This article has been accepted for publication and undergone full peer review but has not been through the copyediting, typesetting, pagination and proofreading process, which may lead to differences between this version and the Version of Record. Please cite this article as doi: 10.1111/1462-2920.13126

Summary

The Crc protein, together with the Hfq protein, participates in catabolite repression in pseudomonads, helping to coordinate metabolism. Little is known about how Crc affects the hierarchy of metabolite assimilation from complex mixtures. Using proton NMR spectroscopy, we carried out comprehensive metabolite profiling of culture supernatants (metabolic footprinting) over the course of growth of both *Pseudomonas putida* and *P. aeruginosa*, and compared the wild-type strains to deletion mutants for *crc*. A complex metabolite consumption hierarchy was observed, which was broadly similar between the two species, although with some important differences, for example in sugar utilisation. The order of metabolite utilisation changed upon inactivation of the *crc* gene, but even in the Crc-null strains some compounds were completely consumed before late metabolites were taken up. This suggests the presence of additional regulatory elements that determine the time and order of consumption of compounds. Unexpectedly, the loss of Crc led both species to excrete acetate and pyruvate as a result of unbalanced growth during exponential phase, compounds that were later consumed in stationary phase. This loss of carbon during growth helps to explain the contribution of the Crc/Hfq regulatory system to evolutionary fitness of pseudomonads.

Introduction

Complex media such as LB (Lysogeny broth) are frequently used to culture bacteria because of their high nutritional value, which allows high growth rates and elevated yields for many bacterial species, including pseudomonads. LB contains tryptone (a tryptic digest of casein) and yeast extract as sources of amino acids, peptides, vitamins and other organic compounds (Sezonov et al., 2007). LB medium generates a strong carbon catabolite repression (CCR) response while cells grow exponentially that allows the preferential assimilation of some carbon sources, thereby optimizing metabolism and growth. In the case of pseudomonads, growth in LB strongly inhibits the expression of genes involved in the assimilation of less-preferred carbon sources such as *n*-alkanes, toluene, xylene, phenol or benzoate (reviewed in Rojo, 2010). When provided as mixtures in a defined medium, amino acids exert a clear CCR effect over the assimilation of sugars and hydrocarbons (Yuste et al., 1998; Hester et al., 2000a). However, several data suggest that not all amino acids are equally preferred. For example, branched-chain amino acids are less preferred than succinate, glucose and several amino acids (Hester et al., 2000a; Hester et al., 2000b; Moreno et al., 2009a). Furthermore, metabolomic analyses directed to monitor the assimilation of amino acids by *Pseudomonas aeruginosa* when cultivated in different complex media showed that cells assimilate the amino acids in a sequential and hierarchical manner. The order of uptake of the diverse amino acids was similar, but not identical, in different complex media analysed, although the general trend observed was that glutamine, asparagine, aspartate, alanine and glutamate were assimilated first, while other amino acids were assimilated at a later stage (Palmer et al., 2007; Behrends et al., 2009; Frimmersdorf et al., 2010; Behrends et al., 2013).

In the case of *P. putida*, the information available on the order of assimilation of the amino acids present in complex media have mostly been inferred from data on gene and protein expression obtained through transcriptomic and proteomic approaches (Moreno et

al., 2009a). These analyses showed that, in cells growing exponentially in LB medium, the Crc regulator has an important role in repressing the expression of genes required for the uptake and/or assimilation of several amino acids, suggesting that proline, alanine, glutamate, glutamine, histidine, arginine, lysine, aspartate and asparagine are preferred over the branched-chain amino acids, threonine, phenylalanine, tyrosine, glycine or serine.

In pseudomonads, CCR is thought to be elicited mainly through a regulatory system based on the Crc and Hfq proteins, and one or more small RNAs that seem to antagonize the effect of these regulatory proteins (Sonnleitner and Blasi, 2014; Madhushani et al., 2015; Moreno et al., 2015). *Pseudomonas aeruginosa* contains only one such sRNA, named CrcZ (Sonnleitner et al., 2009), while *P. putida* harbours CrcZ and an additional sRNA, named CrcY, which is homologous to CrcZ (Moreno et al., 2012). The Crc and Hfq proteins are post-transcriptional regulators that work together to inhibit translation of particular mRNAs that contain an A-rich sequence motif close to the translation initiation site, to which Hfq binds with the help of Crc (Moreno et al., 2009b; Sonnleitner and Blasi, 2014; Madhushani et al., 2015; Moreno et al., 2015). The levels of CrcZ and CrcY are inversely proportional to the strength of the CCR effect. These sRNAs contain several A-rich motifs and, when CCR is not needed, they are believed to form a complex with Hfq, and possibly Crc as well, that renders these proteins unavailable to repress translation initiation. The strong repression exerted by the Crc/Hfq system during exponential growth in LB medium ceases when cells reach the stationary phase of growth (Yuste and Rojo, 2001).

Inactivation of the *crc* gene led to deregulated expression of 134 genes in *P. putida* growing exponentially in LB medium (Moreno et al., 2009a). Interestingly, 28% of these genes are involved in the transport of substrates across the membrane, and 36% have functions related to energy metabolism. Moreover, Crc was recently found to regulate the central metabolic fluxes when cells are cultivated in a defined medium in the presence of succinate and glucose as carbon sources, contributing to organize and optimize metabolism and growth (La Rosa et al., 2015). Much information is available on the Crc

regulon, and many Crc/Hfq regulated genes have been identified (Moreno et al., 2009a; Sonnleitner et al., 2012; Browne et al., 2010), but the information on how Crc mediates the assimilation of the carbon sources present in complex mixtures such as LB medium is still very incomplete. In addition, although gene expression data can be very useful to indicate which compounds may be preferentially metabolized, a definitive proof requires a parallel monitoring of the depletion of the different compounds present in the growth medium. Here we carried out a global metabolic footprint analysis to better understand the hierarchy of assimilation of the compounds present in LB medium by *P. putida* and *P. aeruginosa*, and the role of the Crc/Hfq/CrcZ-CrcY regulatory system in orchestrating this hierarchy.

Results and discussion

Compounds identified in LB medium by NMR

Previous analyses of the composition of LB medium involved a hydrolytic treatment that converted all peptides into free amino acids (Sezonov et al., 2007). In this work we have analysed the composition of LB without any hydrolysis, using an approach based on NMR spectroscopy described earlier (Behrends et al., 2009). As before, we could identify free low-molecular-weight compounds such as amino acids, sugars and organic acids (Supplementary material, Fig. S1). However, in our current study we report absolute (molar) concentrations, as opposed to the relative concentrations that we measured before. NMR gives an untargeted and comprehensive picture of the high-concentration small-molecule metabolites in the media, i.e. those that are potential carbon sources for growth: low concentration metabolites below the NMR detection threshold (which is metabolite-specific, but typically around 0.01 mM) may also have been taken up, but would not be of high importance as C sources for growth. Information on peptides was not obtained, as large peptides, proteins and other macromolecules have relaxation properties

different from the small molecules quantified in this study (Beckonert et al., 2007). There were also some differences between the two batches of LB used to culture the two different species (Supplementary material, Fig. S1), which is not unexpected for an undefined medium.

Comparison of metabolite utilization hierarchies by wild-type P. putida KT2440 and *P. aeruginosa* PAO1

The wild-type *P. putida* KT2440 strain grew exponentially at 30°C (its growth optimum) at a rate of 0.86 ± 0.01 h^{-1} up to a turbidity (A_{600}) above 1, at which point the growth rate started to decline, eventually ceasing at a turbidity close to 4 (Fig. 1A). *Pseudomonas aeruginosa* PAO1 (grown at 37°C) showed a similar growth profile with a slightly higher growth rate during exponential phase (0.96 ± 0.02 h^{-1}, Fig. 1C). To analyse metabolite utilisation and hierarchy, culture supernatants were sampled throughout growth (Fig. 1A, C) and analysed using NMR spectroscopy. Individual metabolites were then quantified by deconvolution, and non-linear (sigmoid) models fitted to the concentration data against time (Fig. S2, Supplementary material). These models allow defining three parameters for each metabolite (Behrends et al., 2009; Behrends et al., 2013; Behrends et al., 2014). The first one, t_{50}, is the time point at which 50% of a given compound has been consumed. The second parameter is the "assimilation time" and indicates the amount of time in which a compound decreases from 75% to 25% of its initial concentration. The combination of these two parameters represents the "uptake window" in which each metabolite is consumed. A third parameter is the "amplitude" of the decrease in concentration of a given metabolite and, when combined with its assimilation time, allows deducing the "uptake rate", which represents the speed at which a metabolite is consumed. We note that depletion of a given compound from the medium does not necessarily imply its complete assimilation. However, the appearance of new compounds in culture supernatants was not detected, and while some organic acids were excreted during exponential growth, these

were consumed at later times (see below). Therefore, depletion of metabolites from the culture medium most likely reflects their assimilation by the cells.

The order of metabolite utilization in *P. aeruginosa* has been described before, on several media (Behrends et al., 2009; Behrends et al., 2013), but this is not the case for *P. putida*, and so we describe the results for *P. putida* in more detail. *Pseudomonas putida* consumed a group of nine metabolites (formate, glucose, succinate, asparagine, glycerol, serine, aspartate, proline and glutamate) in early exponential growth (low t_{50} values), and these were essentially exhausted after 3-4 hours of growth (Figs. 2B, S2, S3). However, the uptake rates within this group clearly differed: glycerol, glutamate, aspartate, proline and serine were consumed faster, while glucose, formate, succinate or asparagine, were consumed at a comparatively slower rate (Figs. 2B, S2, S3). Some compounds were consumed right from the start (formate, glucose, asparagine), while the use of glutamate or aspartate required a lag time of 2 to 2.5 hours that was followed by their fast disappearance from the culture supernatant. The 2.5 h lag for glutamate is noteworthy, given that it was one of the most abundant compounds detected in the LB and, following the lag, it had a fast uptake rate (Figs. 2B, S2, S3). It is worth noting that, although the cells were able to maintain a constant growth rate during exponential phase, the sequential assimilation of the different compounds means that the culture is never under a true steady-state condition.

Once this first group of compounds had been consumed after 3 hours of growth, which allowed cells to reach mid-exponential phase, a second group of several amino acids started to be used (approximately hour 4.5 onwards). In this case, their t_{50} values were rather diverse (Figs. 2B and S3). During late exponential phase (hours 4.5 to 6), alanine, arginine and pyroglutamate were taken up, followed by glycine. The transition from the exponential to the stationary phase of growth (about 6 to 9 hours of culture; Fig. 1A) was characterised by the consumption of leucine, isoleucine, phenylalanine, threonine, valine, tyrosine and methionine, all of which were essentially exhausted by hour 9, corresponding to the start of stationary phase (Fig. 2B and S3). During stationary phase,

the cells continued to consume lysine (which is highly abundant in LB medium) over several hours.

P. putida and *P. aeruginosa* are closely related, and both are considered metabolically versatile copiotrophs. Unsurprisingly, then, there was a broad similarity between their metabolic preferences, as shown by the order of metabolite consumption for the two species (Fig. 2B, 3B). There were, though, a number of clear differences between them (summarised in Fig. 4), which challenges the assumption that the two species will necessarily be physiologically similar in all regards. For example, *P. putida* used serine and proline as preferred carbon sources, taking them up during the first 2-3 hours of growth (Fig. 2B), but these were not utilized by *P. aeruginosa* until late exponential (proline) or stationary phase (serine) (Fig. 3B). Methionine was a less-preferred substrate for *P. putida*, as it was not consumed until stationary phase; however *P. putida* then used all methionine present. *Pseudomonas aeruginosa* assimilated only about one-third of the available methionine, even after 24h. In general, the lipophilic amino acids were more preferred by *P. putida* than by *P. aeruginosa*, as valine, leucine, isoleucine, threonine and tyrosine were all assimilated earlier by *P. putida* than by *P. aeruginosa*; the exception was tryptophan, which was not consumed at all by *P. putida*. The sugar trehalose was also consumed by *P. aeruginosa* but not *P. putida* (Fig. 4 and S3).

Effects of Crc on the hierarchy of consumption of metabolites

Using the global metabolic footprinting approach described here we analysed the behaviour of *P. putida* and *P. aeruginosa* deletion mutants for both the regulatory protein Crc and the regulatory sRNAs (CrcZ for *P. aeruginosa* and CrcZ/CrcY for *P. putida*). The Crc-null derivatives of the two bacterial species had slight growth defects, with 7.5% and 4.2% reductions in exponential growth rates for *P. putida* and *P. aeruginosa*, respectively, although total biomass was comparable after 24h (Fig. 1A, C). In spite of its lower growth rate, the *P. putida* Crc-null strain consumed 22.5% more oxygen during exponential growth than the wild type (Fig. 1B; data not available for *P. aeruginosa*). The *P. putida* KT2440

derivative lacking both CrcZ and CrcY sRNAs, in which CCR is constitutive and very strong (Moreno et al., 2012), showed growth rate and oxygen consumption values very similar to those of the wild type strain (Fig. 1A-B), and the growth rate of the PAO1 derivative lacking the CrcZ sRNA was similar to that of PAO1 (Fig. 1C). These results suggest that Crc favours a more efficient metabolism that leads to a higher growth rate with lower oxygen consumption.

There were also clear effects of *crc* and *crcZ*/*crcZcrcY* mutations on the hierarchy of uptake of substrates both in *P. putida* (Fig 2) and in *P. aeruginosa* (Fig. 3). The results indicate that Crc does indeed affect both rates and orders of compound uptake, and in a fashion that is in most cases consistent with the indirect evidence based on gene expression reported earlier (Moreno et al., 2009a; Sonnleitner et al., 2012). It would be impractical to discuss in depth the behaviour of all substrates for both species, but some cases are worth mentioning. For example, inactivation of the *crc* gene increased the uptake rate of glucose for *P. putida* by 1.7-fold, although assimilation was still slow in comparison to that of other compounds (Fig. 2A-B). However it had little influence on its hierarchy of utilisation. In the CrcZY-null strain, for which Crc-dependent CCR is very strong, glucose consumption was delayed, with t_{50} = 2.8 hours, compared to 1.6 hours for the wild type or the Crc-null strain (Figs. 2C and S3). The increase in rate of glucose uptake in the Crc-null strain and the delay in uptake for the CrcZY-null strain is consistent with reports showing that Crc mediates inhibition of the expression of the genes coding for the OprB1 porin and the GstABCD transporter, involved in glucose uptake (Moreno et al., 2009a; La Rosa et al., 2015; del Castillo et al., 2007; del Castillo et al., 2008). It is worth noting that, in contrast to the general view that glucose is not a preferred compound for *P. putida*, our results show that this sugar is co-metabolized during the first hours of exponential growth, despite clear – albeit partial – repression by Crc. Clearly, glucose is a more highly preferred carbon source for *P. putida* than *P. aeruginosa*, which exhibited a different behaviour. In the wild type strain, glucose was not consumed during exponential growth, and concentrations actually increased after entry to stationary phase (hence t_{50}

value could not be calculated), presumably because of hydrolysis of trehalose into two glucose units by the periplasmic trehalase encoded by *treA* (PA2416). Glucose concentration peaked after 14 hours of growth (Fig. S4), followed by a drop as the cells switch to glucose assimilation. Conversely, the Crc-null strain, and to a lesser extent the CrcZ-null strain, consumed glucose during exponential growth (Fig. S4).

Inactivation of the *crc* gene had a clear impact on the hierarchy and speed of assimilation of several amino acids, leading to altered t_{50} values and uptake rates for most of them. In *P. putida,* asparagine, proline, alanine, glycine, phenylalanine, pyroglutamate and tyrosine were consumed earlier and/or faster by the Crc-null strain (Fig. 2), which is consistent with previous reports showing that the expression of genes involved in the transport and/or assimilation of most of these amino acids is inhibited by Crc (Moreno et al., 2009a). Asparagine was consumed earlier and faster by the Crc-null strain than by the wild type, and it was first converted into extracellular aspartate, as shown by the increase in aspartate concentrations that were inversely correlated to asparagine levels (Fig. S5). Aspartate was consumed when asparagine was depleted. Crc seemed to have little influence on the assimilation of glutamate, aspartate, arginine, lysine, methionine, threonine, serine, valine, leucine and isoleucine. The case of the branched-chain amino acids leucine, isoleucine and valine is noteworthy. In *P. putida*, their consumption did not start until cells reached the stationary phase of growth, indicating that they are non-preferred compounds. The Crc protein has been identified as a negative co-regulator of the genes involved in their transport and assimilation (Moreno et al., 2009a; Hester et al., 2000a; Hester et al., 2000b). However, inactivation of the *crc* gene in *P. putida* did not improve the depletion of any of these three amino acids, suggesting that other still unidentified factors inhibit their use. Finally, the pattern of consumption of amino acids of the strain lacking the CrcZ and CrcY sRNAs was in most cases very similar to that of the wild type strain, although assimilation of asparagine, proline and pyroglutamate was delayed (Fig. 2), presumably caused by a strong Crc-dependent repression.

The *P. aeruginosa* Crc-null strain also showed modifications to the hierarchy and speed of consumption of several amino acids, but clear differences were observed when compared to *P. putida*. Alanine, pyroglutamate, phenylalanine, tyrosine, isoleucine and leucine were assimilated earlier by the Crc-null strain, while consumption of other amino acids was not affected, or delayed. Many of these changes were not observed in the strain lacking the CrcZ sRNA, although the consumption of some substrates was accelerated (glycerol, pyroglutamate, serine, or proline), while that of tyrosine was delayed. Differences between the CrcZ-null and the wild type strain were, however, not great.

The most striking overall result is that, even in Crc-null mutants, there is still a marked hierarchy of metabolite utilization, stretching from immediate uptake, to metabolites that are only taken up in stationary phase (Figs. 2, 3, and S3), suggesting that there is an extensive catabolite repression operating even if Crc is absent. It seems that the Crc protein accounts for only part of the regulatory control of metabolite assimilation hierarchies in *Pseudomonas*: most metabolites have little change between the different mutants, compared to the overall spread of t_{50} values. Some do alter, e.g. succinate is a preferred substrate for *P. aeruginosa*, as it was taken up with asparagine as the earliest-used compound, but its t_{50} changed from about 1.6 to 3.6 h for the *crc* mutant, such that it was assimilated together with lactate, and after both asparagine and glycerol were consumed (Figs. 3 and S3).

Inactivation of the crc gene leads to acetate and pyruvate secretion

An unexpected phenotype was that *crc* mutants of both species excreted large amounts of the organic acids acetate and pyruvate during exponential growth, and then consumed them again during stationary phase (Fig. 5). The *P. putida crc* mutant was a stronger pyruvate than acetate producer, with maximum levels of around 3.5 mM pyruvate compared to 1.5 mM acetate; the situation was reversed for the *P. aeruginosa crc* mutant, with maximum levels of around 0.8 and 3 mM pyruvate and acetate, respectively (Fig. 5). We believe that these observed differences in organic acid excretion are primarily the

result of differences in the metabolism of the two bacterial species, but we cannot rule out that some of the disparities may also be affected by the concentration of some of the compounds present in the batches of LB medium used in each case (e.g., lactate; Fig. S1). The *P. aeruginosa crcZ* mutant also excreted some pyruvate and acetate, although not as much, while the *P. putida* CrcZY-null strain behaved like the wild type (Fig. 5).

Why did the bacteria excrete these compounds? Pyruvate excretion has been previously observed in several *P. aeruginosa* strains under conditions of metabolic imbalance. For example, strain PA14 secretes pyruvate in the late stationary phase under aerobic/microaerobic growth conditions, probably to balance redox conditions (Price-Whelan et al., 2007). Interestingly, when growing exponentially in LB, the *P. putida* Crc-null strain showed a higher expression of several genes that transform different compounds to pyruvate, as for example those coding for the enzymes transforming serine into pyruvate (Sda2), sugars to pyruvate (Entner-Doudoroff pathway), or oxaloacetate to pyruvate (OadA) (Moreno et al., 2009a). The Crc-null strain also consumed alanine earlier, an abundant amino acid that is directly transformed to pyruvate by alanine transaminase. The excretion of acetate and pyruvate by the *P. putida* and *P. aeruginosa* Crc-null strains may therefore be a consequence of the deregulated expression of several key genes involved in the assimilation of carbon sources. This would produce a metabolic imbalance that leads to the accumulation of intermediates such as acetate and pyruvate, which leak out of the cell during growth. These compounds were recovered and consumed again when cells entered the stationary phase of growth.

Crc mutants have only a small growth defect for both *P. aeruginosa* and *P. putida*, as shown in our current study (Fig. 1). Nonetheless, competition experiments show a clear decline in the number of *crc*-mutant cells in mixed mutant/wild type populations, indicating a reduction in evolutionary fitness when Crc is not present (Moreno et al., 2009a). The excretion of organic acids will contribute to that loss of fitness, over and above changes in growth rate: clearly, when grown in mixed populations, Crc-deficient mutants will lose

carbon in the form of organic acids to wild-type cells, which will help to maintain the Crc/Hfq/CrcZY system in natural populations.

Conclusions

Wild-type *P. putida* and *P. aeruginosa* both make a sequential use of the different compounds available, although the hierarchy of consumption showed some notable differences between the two species. Inactivating the *crc* gene had only a minor effect on growth, but increased oxygen consumption in *P. putida* by more than a fifth, indicating reduced metabolic efficiency. Metabolic profiling confirmed that the order of utilization of different metabolites did change significantly relative to that seen for the wild type strain. In addition, the Crc-null strains unexpectedly excreted significant amounts of pyruvate and acetate during exponential growth. These results strongly suggest that lack of Crc leads to an unbalanced metabolism, consistent with earlier studies (Moreno et al., 2009a; La Rosa et al., 2014; La Rosa et al., 2015), and emphasise the key role of the Crc protein in helping *Pseudomonas* to adapt to and get the most from an environment that is in constant change due to the sequential consumption of the available substrates. Nevertheless, it should be stressed that although the absence of Crc altered the use of several compounds, these were still consumed in a sequential and hierarchical manner. The reasons underlying this Crc-independent hierarchy are at present unknown, but suggest that other regulatory elements are still present that control the use of carbon sources. For example, although the Crc-null strain lacks Crc, it still contains the Hfq protein, which might be responsible for at least part of the new hierarchy observed. In fact, current evidence suggests that Crc potentiates the repressive action of Hfq, stabilizing the Hfq-RNA complexes formed at A-rich sites (Sonnleitner and Blasi, 2014; Madhushani et al., 2015; Moreno et al., 2015). Additional Crc-independent CCR systems have been described in *P. putida*, such as those involving the Pts^{Ntr} proteins (Cases et al., 2001; Pflüger-Grau and Görke, 2010) and the

Cyo terminal oxidase (Dinamarca et al., 2002; Morales et al., 2006), although their relevance seems to be smaller and probably cannot explain the assimilation hierarchy observed when Crc is inactivated. There may well be still uncharacterized regulatory systems that help to coordinate metabolism in pseudomonads.

Experimental procedures

Bacterial strains and culture media

P. putida strains were cultivated at 30°C with vigorous shaking in LB medium (tryptone, 10 g l^{-1}; yeast extract, 5 g l^{-1}; NaCl, 10 g l^{-1}). The *P. putida* strains used were KT2440 (wild type; Franklin et al., 1981), KTCRC (a KT2440 derivative containing an inactivated *crc* allele; Hernández-Arranz et al., 2013), and KT2440-ZY, which derives from KT2440 by deletion of the *crcZ* and *crcY* genes (La Rosa et al., 2015). *Pseudomonas aeruginosa* strains were cultivated at 37°C with vigorous shaking in LB medium (tryptone, 10 g l^{-1}; yeast extract, 5 g l^{-1}; NaCl, 5 g l^{-1}). The *P. aeruginosa* strains used were PAO1 (wild type), PAO6673 (a PAO1 derivative containing an inactivated *crc* allele; Sonnleitner et al., 2009), PAO6679 (a PAO1 derivative containing an inactivated *crcZ* allele; Sonnleitner et al., 2009). Antibiotics were added when needed at the following concentrations: tetracycline 10 µg ml^{-1} and gentamicin 10 µg ml^{-1}.

Measurement of oxygen consumption

P. putida strains KT2440, KTCRC and KT2440-ZY were grown in 50 ml flasks with strong aeration until cultures reached to a turbidity (A_{600}) of 0.6. At this point, 0.5 ml of the cultures were diluted 1:2 with preheated fresh medium and the respiration rate measured using an oxygraph (Hansatech, United Kingdom) fitted with a Clark's type oxygen electrode, according to the manufacturer's instructions (Sevilla et al., 2013). The dry weight of the

samples was used as the reference parameter. The consumption rate is expressed as mmol O_2 consumed per mg of cell dry weight per hour.

Metabolite footprinting (NMR sampling)

Cells were inoculated using two different batches of LB medium and cultured overnight at 30ºC (*P. putida*) or 37°C (*P. aeruginosa)*. These cultures were used to inoculate three separate 250 ml flasks containing 50 ml of fresh LB, up to a turbidity (A_{600}) of 0.03. Cells were allowed to grow with vigorous aeration and 1 ml aliquots were sampled successively throughout growth (0, 1, 1.5, 2, 2.5, 3, 3.5, 4, 5, 6, 7, 8, 10, 12, 14, 24 hours after inoculation for *P. putida,* and 0, 1.5, 3, 4, 5, 6, 7, 8, 10, 12, 14, 24 hours after inoculation for *P. aeruginosa*). The turbidity was recorded for each sample, and 0.7 ml of cell suspension then centrifuged at 16000 x *g* for 5 minutes at room temperature. The supernatant (0.6 ml) was collected and stored at -80°C until NMR analysis.

Nuclear magnetic resonance spectroscopy

The samples were defrosted at room temperature and 520 µl of supernatant were mixed with 130 µl of NMR buffer (0.25 M phosphate buffer, pH 7, in 100% ^2H_2O containing 0.2 mM 2,2-dimethyl-2-silapentane-d_6-5-sulfonic acid (DSS), which served as both internal chemical shift reference and concentration standard). Samples were centrifuged at 16000 x *g* for 5 minutes at room temperature and 600 µl of the supernatant were transferred to SampleJet 5 mm NMR tubes. Spectra were acquired on a Bruker Avance DRX600 NMR spectrometer (Bruker BioSpin, Rheinstetten, Germany), with a magnetic field strength of 14.1 T and a resulting ^1H resonance frequency of 600 MHz, equipped with a 5-mm inverse probe. Samples were introduced using a SampleJet autosampler. Spectra were acquired following the approach described (Beckonert et al., 2007). Briefly, a one-dimensional NOESY pulse sequence was used for water suppression; data were acquired into 32 K data points over a spectral width of 12 kHz, with 8 dummy scans and 128 scans per sample, and an additional longitudinal relaxation recovery delay of 3.5 s per scan, giving a

total recycle time of 5 s. After acquisition, the spectra were processed in NMR Suite 8.0 (Chenomx, Inc., Edmonton, Alberta, Canada), including Fourier transformation and manual baseline correction and phasing. We have previously assigned peaks in LB medium (Behrends et al., 2009); the peaks were fitted in a 'targeted profiling' approach (Weljie et al., 2006) to determine concentrations using the standard Chenomx spectral database.

Non-linear fitting of metabolites concentration

Nonlinear regression of the data against time was carried out as described (Behrends et al., 2009), although using the fitted compound concentration data rather than simple spectral integrals. Briefly, we fitted a four-parameter sigmoid curve (equation 1):

$$y = A/[1 + e^{-(x-B)/C}] + D \quad (1)$$

These parameters have meaningful biological interpretations: in particular, B is a 'half life' parameter (t_{50}) that represents the time at which half of a metabolite has been consumed (i.e. the inflection point of the curve). C is a 'width' parameter, or uptake window, over which most of the metabolite assimilation takes place (and is therefore inversely related to uptake rate). Cut-offs were imposed for B (1 to 24 h), C (0 to 3 h), and overall fit ($R^2 > 0.96$). The "uptake rate" (in mmol h^{-1}) for each metabolite was defined by dividing half of the initial concentration by the assimilation time, and represents the speed of consumption of a compound during the uptake window (when its concentration decreases from 75% to the 25% of the initial value).

Acknowledgements

We are grateful to Renata Moreno and Emma Sevilla for helpful discussions and to Luis Yuste for excellent technical assistance. Ruggero La Rosa was a recipient of a predoctoral fellowship from the La Caixa Foundation, and of a Short-Term EMBO Fellowship. This

work was funded by grants BFU2012-32797 from the Spanish Ministry of Economy and Competitiveness (Plan Nacional I+D+i).

References

Beckonert, O., Keun, H.C., Ebbels, T.M., Bundy, J., Holmes, E., Lindon, J.C., and Nicholson, J.K. (2007) Metabolic profiling, metabolomic and metabonomic procedures for NMR spectroscopy of urine, plasma, serum and tissue extracts. *Nat Protoc* **2**: 2692-2703.

Behrends, V., Ebbels, T.M., Williams, H.D., and Bundy, J.G. (2009) Time-resolved metabolic footprinting for nonlinear modeling of bacterial substrate utilization. *Appl Environ Microbiol* **75**: 2453-2463.

Behrends, V., Bell, T.J., Liebeke, M., Cordes-Blauert, A., Ashraf, S.N., Nair, C. et al. (2013) Metabolite profiling to characterize disease-related bacteria: gluconate excretion by *Pseudomonas aeruginosa* mutants and clinical isolates from cystic fibrosis patients. *J Biol Chem* **288**: 15098-15109.

Behrends, V., Williams, H.D., and Bundy, J.G. (2014) Metabolic footprinting: extracellular metabolomic analysis. *Methods Mol Biol* **1149**: 281-292.

Browne, P., Barret, M., O'Gara, F., and Morrissey, J.P. (2010) Computational prediction of the Crc regulon identifies genus-wide and species-specific targets of catabolite repression control in *Pseudomonas* bacteria. *BMC Microbiol* **10**: 300.

Cases, I., Velázquez, F., and de Lorenzo, V. (2001) Role of *ptsO* in carbon-mediated inhibition of the *Pu* promoter belonging to the pWW0 *Pseudomonas putida* plasmid. *J Bacteriol* **183**: 5128-5133.

del Castillo, T., Ramos, J.L., Rodríguez-Hervá, J.J., Fuhrer, T., Sauer, U., and Duque, E. (2007) Convergent peripheral pathways catalyze initial glucose catabolism in *Pseudomonas putida*: genomic and flux analysis. *J Bacteriol* **189**: 5142-5152.

del Castillo, T., Duque, E., and Ramos, J.L. (2008) A set of activators and repressors control peripheral glucose pathways in *Pseudomonas putida* to yield a common central intermediate. *J Bacteriol* **190**: 2331-2339.

Dinamarca, M.A., Ruiz-Manzano, A., and Rojo, F. (2002) Inactivation of cytochrome *o* ubiquinol oxidase relieves catabolic repression of the *Pseudomonas putida* GPo1 alkane degradation pathway. *J Bacteriol* **184**: 3785-3793.

Franklin, F.C., Bagdasarian, M., Bagdasarian, M.M., and Timmis, K.N. (1981) Molecular and functional analysis of the TOL plasmid pWWO from *Pseudomonas putida* and cloning of genes for the entire regulated aromatic ring *meta* cleavage pathway. *Proc Nat Acad Sci USA* **78**: 7458-7462.

Frimmersdorf, E., Horatzek, S., Pelnikevich, A., Wiehlmann, L., and Schomburg, D. (2010) How *Pseudomonas aeruginosa* adapts to various environments: a metabolomic approach. *Environ Microbiol* **12**: 1734-1747.

Hernández-Arranz, S., Moreno, R., and Rojo, F. (2013) The translational repressor Crc controls the *Pseudomonas putida* benzoate and alkane catabolic pathways using a multi-tier regulation strategy. *Environ Microbiol* **15**: 227-241.

Hester, K.L., Lehman, J., Najar, F., Song, L., Roe, B.A., MacGregor, C.H. et al. (2000a) Crc is involved in catabolite repression control of the *bkd* operons of *Pseudomonas putida* and *Pseudomonas aeruginosa*. *J Bacteriol* **182**: 1144-1149.

Hester, K.L., Madhusudhan, K.T., and Sokatch, J.R. (2000b) Catabolite repression control by *crc* in 2xYT medium is mediated by posttranscriptional regulation of *bkdR* expression in *Pseudomonas putida*. *J Bacteriol* **182**: 1150-1153.

La Rosa, R., de la Peña, F., Prieto, M.A., and Rojo, F. (2014) The Crc protein inhibits the production of polyhydroxyalkanoates in *Pseudomonas putida* under balanced carbon/nitrogen growth conditions. *Environ Microbiol* **16**: 278-290.

La Rosa, R., Nogales, J., and Rojo, F. (2015) The Crc/CrcZ-CrcY global regulatory system helps the integration of gluconeogenic and glycolytic metabolism in *Pseudomonas putida*. *Environ Microbiol*, **17**: 3362–3378 .

Madhushani, A., del Peso-Santos, T., Moreno, R., Rojo, F., and Shingler, V. (2015) Transcriptional and translational control through the 5'-leader region of the *dmpR* master regulatory gene of phenol metabolism. *Environ Microbiol* **17**: 119-133.

Morales, G., Ugidos, A., and Rojo, F. (2006) Inactivation of the *Pseudomonas putida* cytochrome *o* ubiquinol oxidase leads to a significant change in the transcriptome and to increased expression of the CIO and *cbb3*-1 terminal oxidases. *Environ Microbiol* **8**: 1764-1774.

Moreno, R., Martínez-Gomariz, M., Yuste, L., Gil, C., and Rojo, F. (2009a) The *Pseudomonas putida* Crc global regulator controls the hierarchical assimilation of amino acids in a complete medium: evidence from proteomic and genomic analyses. *Proteomics* **9**: 2910-2928.

Moreno, R., Marzi, S., Romby, P., and Rojo, F. (2009b) The Crc global regulator binds to an unpaired A-rich motif at the *Pseudomonas putida alkS* mRNA coding sequence and inhibits translation initiation *Nucleic Acids Res* **37**: 7678-7690.

Moreno, R., Fonseca, P., and Rojo, F. (2012) Two small RNAs, CrcY and CrcZ, act in concert to sequester the Crc global regulator in *Pseudomonas putida*, modulating catabolite repression. *Mol Microbiol* **83**: 24-40.

Moreno, R., Hernández-Arranz, S., La Rosa, R., Yuste, L., Madhushani, A., Shingler, V., and Rojo, F. (2015) The Crc and Hfq proteins of *Pseudomonas putida* cooperate in catabolite repression and formation of ribonucleic acid complexes with specific target motifs. *Environ Microbiol* **17**: 105-118.

Palmer, K.L., Aye, L.M., and Whiteley, M. (2007) Nutritional cues control *Pseudomonas aeruginosa* multicellular behavior in cystic fibrosis sputum. *J Bacteriol* **189**: 8079-8087.

Pflüger-Grau, K., and Görke, B. (2010) Regulatory roles of the bacterial nitrogen-related phosphotransferase system. *Trends Microbiol* **18**: 205-214.

Price-Whelan, A., Dietrich, L.E., and Newman, D.K. (2007) Pyocyanin alters redox homeostasis and carbon flux through central metabolic pathways in *Pseudomonas aeruginosa* PA14. *J Bacteriol* **189**: 6372-6381.

Rojo, F. (2010) Carbon catabolite repression in *Pseudomonas*: optimizing metabolic versatility and interactions with the environment. *FEMS Microbiol Rev* **34**: 658-684.

Sevilla, E., Alvarez-Ortega, C., Krell, T., and Rojo, F. (2013) The *Pseudomonas putida* HskA hybrid sensor kinase responds to redox signals and contributes to the adaptation of the electron transport chain composition in response to oxygen availability. *Environ Microbiol Rep* **5**: 825-834.

Sezonov, G., Joseleau-Petit, D., and D'Ari, R. (2007) *Escherichia coli* physiology in Luria-Bertani broth. *J Bacteriol* **189**: 8746-8749.

Sonnleitner, E., Abdou, L., and Haas, D. (2009) Small RNA as global regulator of carbon catabolite repression in *Pseudomonas aeruginosa*. *Proc Natl Acad Sci USA* **106**: 21866-21871.

Sonnleitner, E., Valentini, M., Wenner, N., Haichar, F.Z., Haas, D., and Lapouge, K. (2012) Novel targets of the CbrAB/Crc carbon catabolite control system revealed by transcript abundance in *Pseudomonas aeruginosa*. *PloS one* **7**: e44637.

Sonnleitner, E., and Blasi, U. (2014) Regulation of Hfq by the RNA CrcZ in *Pseudomonas aeruginosa* carbon catabolite repression. *PLoS Genet* **10**: e1004440.

Weljie, A.M., Newton, J., Mercier, P., Carlson, E., and Slupsky, C.M. (2006) Targeted profiling: quantitative analysis of 1H NMR metabolomics data. *Anal Chem* **78**: 4430-4442.

Yuste, L., Canosa, I., and Rojo, F. (1998) Carbon-source-dependent expression of the *PalkB* promoter from the *Pseudomonas oleovorans* alkane degradation pathway. *J Bacteriol* **180**: 5218-5226.

Yuste, L., and Rojo, F. (2001) Role of the *crc* gene in catabolic repression of the *Pseudomonas putida* GPo1 alkane degradation pathway. *J Bacteriol* **183**: 6197-6206.

Figure legends

Figure 1. Influence of the Crc regulatory protein, and of the sRNAs CrcZ (*P. aeruginosa*) or CrcZ/CrcY (*P. putida*), on the growth rate and oxygen consumption of *P. putida* and *P. aeruginosa* cultivated in LB medium. (**A**) *P. putida* strains KT2440 (wild type, black line, indicated as "wt"), KTCRC (Crc-null derivative of KT2440; red line, indicated as "*crc*") and KT2440-ZY (a KT2440 derivative lacking both *crcZ* and *crcY*, grey line, indicated as "*zy*") and (**C**) *P. aeruginosa* strains PAO1 (wild type, black line, indicated as "wt"), PAO6673 (Crc-null derivative of PAO1; red line, indicated as "*crc*") and PAO6679 (CrcZ-null derivative of PAO1, grey line, indicated as "*crcZ*"), were cultivated in LB medium for 24 hours. Growth was followed by measuring turbidity at 600 nm. Black bars indicate the standard deviation. Growth rate (h^{-1}) of the strains during exponential phase is indicated in the grey box; values correspond to the mean ± the standard deviation of three independent measurements. The differences in growth rate between the wild type and the *crc*-null strains were statistically significant (*P* values of < 0.001 and < 0.05 for *P. putida* and *P. aeruginosa*, respectively). Green arrows indicate the time points at which samples of supernatant were collected for NMR analyses. (**B**) Specific oxygen consumption of the *P. putida* strains during mid exponential phase (A_{600} = 0.6). Values correspond to the mean ± the standard deviation of three measurements and are indicated as mmol $mgCDW^{-1}$ h^{-1}. The asterisks indicate that a significant difference exists between the samples compared (in brackets), with a P value of ≤ 0.007.

Figure 2. Uptake parameters for the compounds assimilated by *P. putida*. Dots (blue or grey) indicate the t_{50} value (time at which the concentration of the metabolite has decreased to 50% of the initial value) for each compound, while circles (black or grey) represent the speed of assimilation (time needed to detect a reduction in the compound concentration from 75% to 25% of the initial value). The relative amount of each

compound, expressed as mM relative to the DSS standard, is indicated below the corresponding dot (Y-axis in mM; the area of the rectangle is proportional to the concentration value). (**A**) Plot corresponding to *P. putida* KTCRC (Crc-null derivative of KT2440, indicated as "*crc*"). (**B**) Plot corresponding to *P. putida* KT2440 (wild type, indicated as "wt"), (**C**) Plot corresponding to KT2440-ZY (a KT2440 derivative lacking both *crcZ* and *crcY*, indicated as "*zy*").

Figure 3. Uptake parameters for the compounds assimilated by *P. aeruginosa*. Dots (blue or grey) indicate the t_{50} value (time at which the concentration of the metabolite has decreased to 50% of the initial value) for each compound, while the circles (black or grey) represent the speed of assimilation (time needed to detect a reduction in the compound concentration from 75% to 25% of the initial value). The relative amount of each compound, expressed as mM relative to the DSS standard, is indicated below the corresponding dot (Y-axis in mM; the area of the rectangle is proportional to the concentration value). (**A**) Plot corresponding to *P. aeruginosa* PAO6673 (Crc-null derivative of PAO1, indicated as "*crc*"). (**B**) Plot corresponding to *P. aeruginosa* PAO1 (wild type, indicated as "wt"), (**C**) Plot corresponding to PAO6679 (CrcZ-null derivative of PAO1, indicated as "*crcZ*").

Figure 4. Comparison of the hierarchy of assimilation (t_{50} values) for different compounds in *P. putida* (blue line) and *P. aeruginosa* (green line). Only differences higher than ± 1.5 hours were considered as phenotypically significant. The black circles indicate the compounds for which the t_{50} values differ in the two species. Note that trehalose was not assimilated by *P. putida*.

Figure 5. Influence of the Crc/CrcZ(Y) regulatory system on the excretion of acetate and pyruvate. Transient secretion of acetate (**A**, **D**) and pyruvate (**B**, **E**), as revealed by NMR analyses, by the following bacterial strains when cultivated in LB medium: (**A**-**B**) KT2440

(wild type, blue line, indicated as "wt"), KTCRC (Crc-null derivative of KT2440, red line, indicated as "*crc*"), KT2440-ZY (CrcZ- and CrcY-null derivative of KT2440, green line, indicated as "*zy*"); (**D**-**E**) PAO1 (wild type, blue line, indicated as "wt"), PAO6673 (Crc-null derivative of PAO1, red line, indicated as "*crc*"), and PAO6679 (CrcZ-null derivative of PAO1, green line, indicated as "*crcZ*"). Concentrations are indicated in mM, relative to that of the DSS internal standard. (**C**, **F**) Secretion of acetate (green line) or pyruvate (red line) by the Crc-null strains *P. putida* KTCRC (**C**) and *P. aeruginosa* PAO6673 (**F**) along the growth curve. Values were normalized by subtracting the initial concentration of acetate and pyruvate in the culture medium and referring the values obtained to the amount of cells (turbidity at 600 nm) present at each time-point; values are indicated as relative µmol OD^{-1} h^{-1}. The growth curve of the Crc-null strains is also represented for comparison (grey lines). Error bars represent the standard deviation (SD) of the mean.

Supplementary material

Figure S1. Compounds detected in the LB medium. Free amino acids and organic acids detected in the LB medium batches used to cultivate *P. putida* (**A**) and *P. aeruginosa* (**B**), grouped according to their chemical characteristics. Nine replicas of each batch of LB were analysed using NMR spectroscopy. Concentrations represent integral values of characteristic resonances relative to the internal standard DSS. Error bars represent the standard deviation (SD) of the mean.

Figure S2. Consumption of amino acids and organic acids during growth of *P. putida* in LB medium, and influence of the Crc/CrcZ-CrcY regulatory system. Curves represent the sigmoid model fits of metabolites concentration. (**A**) Use of organic acids during exponential growth (between 0 and 6 hours of growth). (**B**, **C**) Use of amino acids during exponential growth (**B**; between 0 and 6 hours of growth), or upon entry into stationary

phase (**C**; between 6 and 24 hours of growth). The indicated concentrations represent the integral values of the characteristic resonances for each compound relative to the internal standard DSS. The *P. putida* strains used were KT2440 (wild type, indicated as "wt"), KTCRC (Crc-null derivative of KT2440, indicated as "*crc*") and KT2440-ZY (a KT2440 derivative lacking both *crcZ* and *crcY*, indicated as "*zy*").

Figure S3. Parameters for the assimilation of the detected compounds. Heat maps of the "t_{50}" values (time at which the concentration has changed by half, indicated in hours), "assimilation times" (time needed to detect a decrease in the relative concentration from 75% to 25% of the starting value, in hours), and "uptake rates" (indicated as mmol h^{-1}), ordered from the highest to the lowest (t_{50} and assimilation time) and from the lowest to the highest (uptake rate). Values derive from the sigmoid fits of concentration data, and correspond to the decrease in concentration of each compound from the 75% to 25% of its initial value, relative to the time period of the decrease. (**A**) Values for *P. putida* strains KT2440 (wild type, indicated as "wt"), KTCRC (Crc-null derivative of KT2440, indicated as "*crc*") and KT2440-ZY (CrcZ- and CrcY-null derivative of KT2440, indicated as "*zy*"). (**B**) Values for *P. aeruginosa* strains PAO1 (wild type, indicated as "wt"), PAO6673 (Crc-null derivative of PAO1, indicated as "*crc*"), and PAO6679 (CrcZ-null derivative of PAO1, indicated as "*crcZ*").

Figure S4. Assimilation of glucose and trehalose during growth of *P. aeruginosa* and influence of the Crc/CrcZ regulatory system. Transient secretion of glucose (**A**) and assimilation of trehalose (**B**), as revealed by NMR analyses of culture supernatants of the *P. aeruginosa* strains PAO1 (wild type, blue line, indicated as "wt"), PAO6673 (Crc-null derivative of PAO1, red line, indicated as "*crc*"), and PAO6679 (CrcZ-null derivative of PAO1, green line, indicated as "*crcZ*"), cultivated in LB medium. (**C**) Comparison of glucose (green line) and trehalose (grey line) concentrations detected in the culture supernatants of *P. aeruginosa* PAO1 when cultivated in LB medium. Concentrations are

indicated in mM relative to that of the DSS internal standard. Error bars represent the standard deviation (SD) of the mean.

Figure S5. Assimilation of asparagine and aspartate during growth of *P. putida* and *P. aeruginosa* in LB medium, and influence of the Crc/CrcZ-CrcY regulatory system. The relative amounts of asparagine and aspartate in culture supernatants were determined by NMR analyses. Concentrations are indicated in mM relative to that of the DSS internal standard. Error bars represent the standard deviation (SD) of the mean. The bacterial strains used are those indicated in Figure S3.

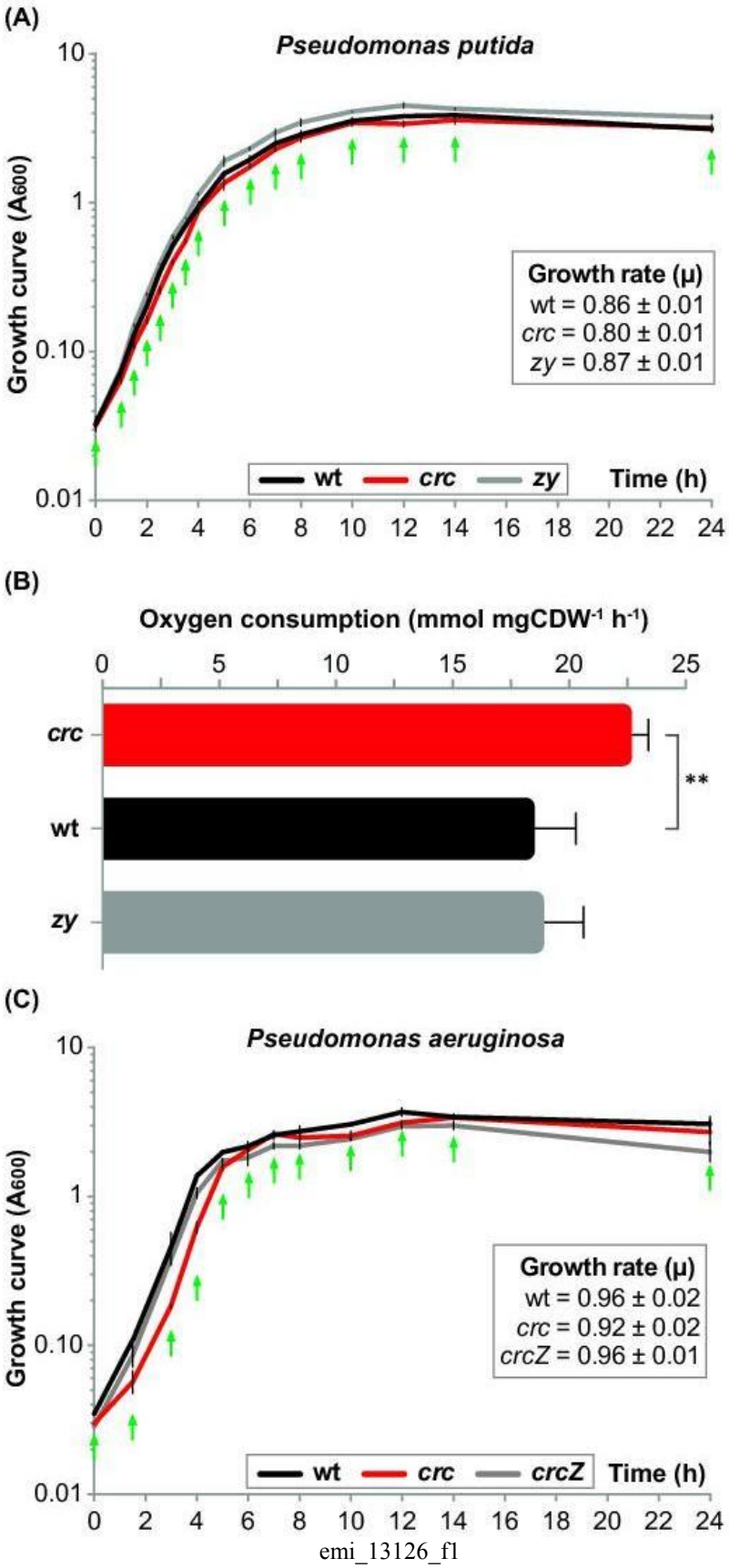

emi_13126_f1

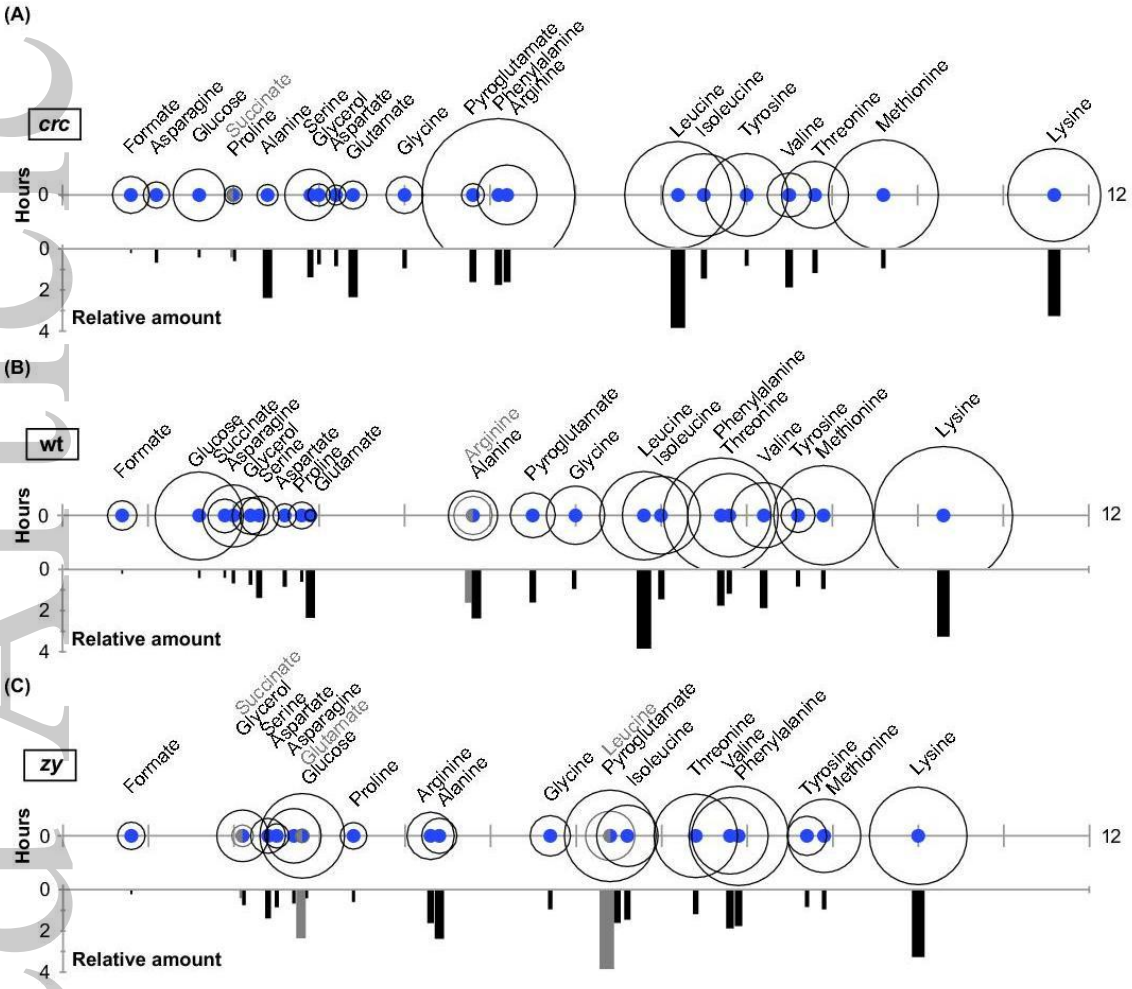

emi_13126_f2

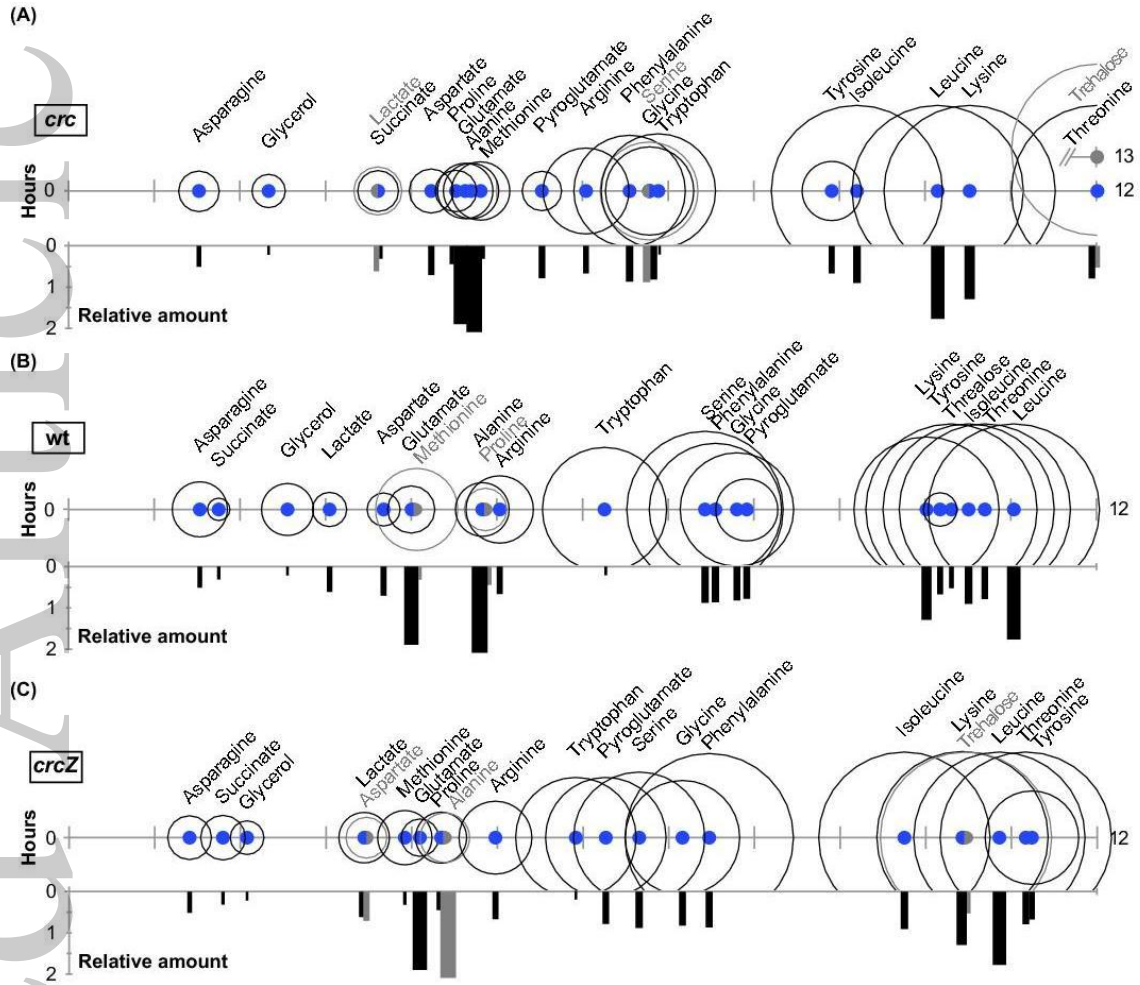

emi_13126_f3

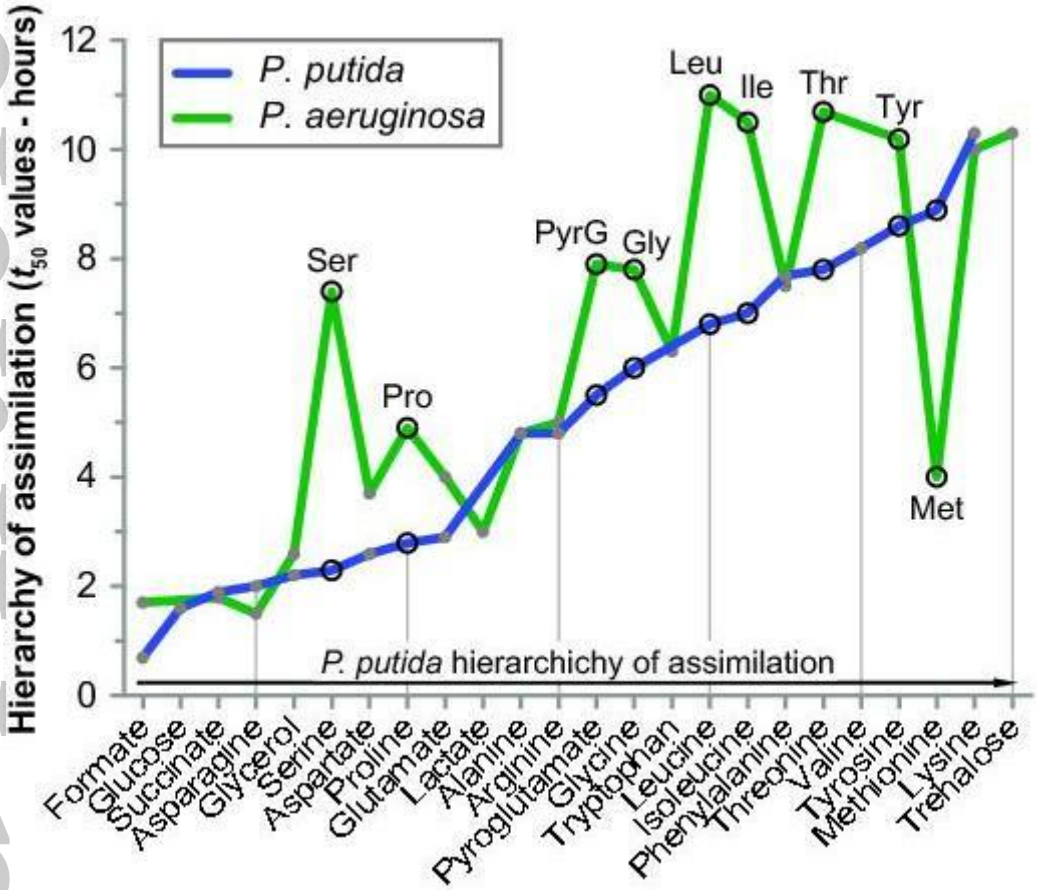

emi_13126_f4

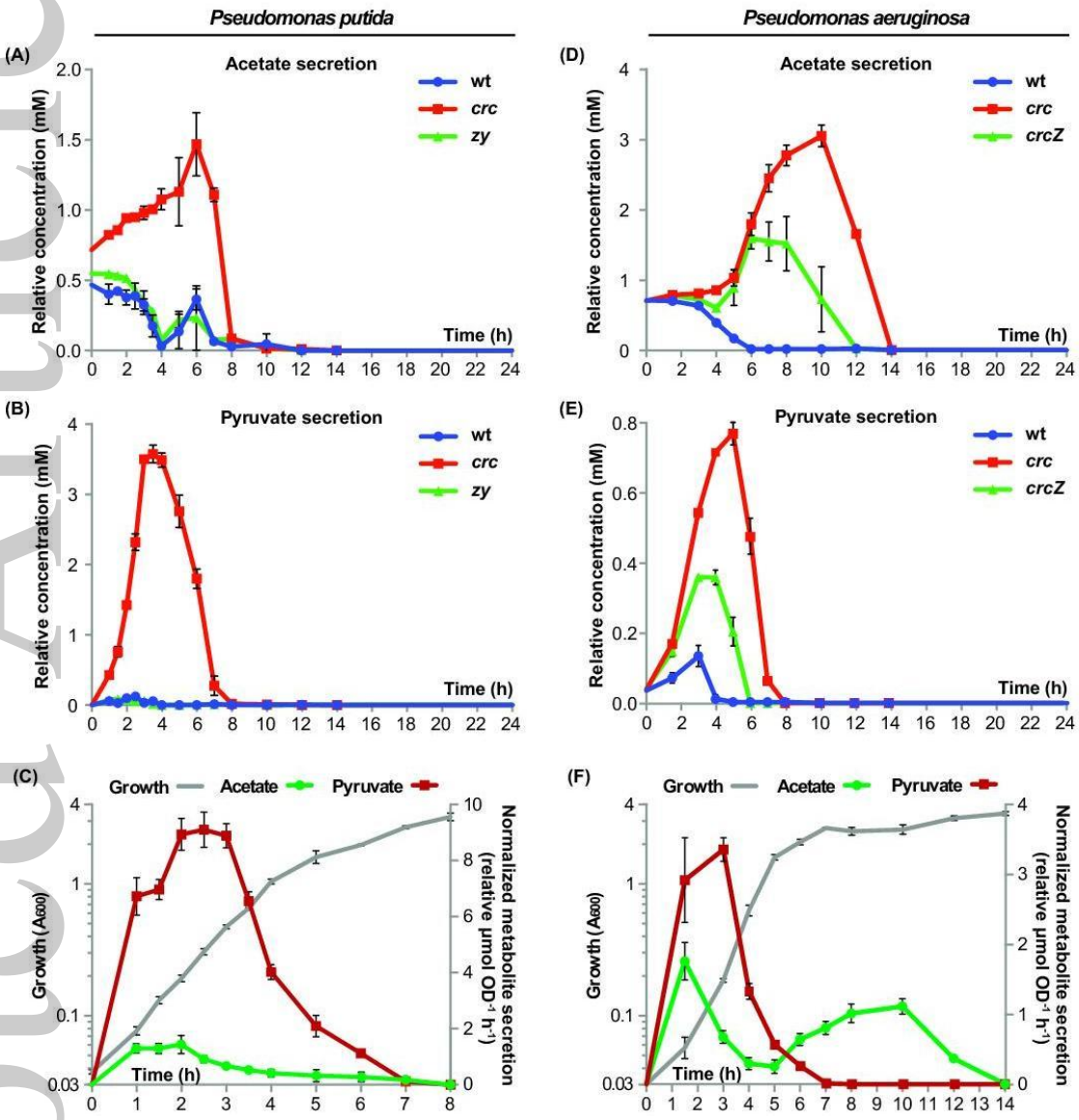

emi_13126_f5